Reference: *Biol. Bull.* **225:** 113–123. (October 2013)

An Externally Brooding Acorn Worm (Hemichordata, Enteropneusta, Torquaratoridae) from the Russian Arctic

KAREN J. OSBORN[1,*], ANDREY V. GEBRUK[2], ANTONINA ROGACHEVA[2], AND NICHOLAS D. HOLLAND[3]

[1]*Department of Invertebrate Zoology, Smithsonian Institution, National Museum of Natural History, Washington, DC 20013-7012;* [2]*P. P. Shirshov Institute of Oceanology, Russian Academy of Sciences, Moscow 117997, Russia; and* [3]*Marine Biology Research Division, Scripps Institution of Oceanography, University of California at San Diego, La Jolla, California 92093*

Abstract. A single specimen of a previously undescribed acorn worm in the family Torquaratoridae was trawled from a bottom depth of about 350 m in the Kara Sea (Russian Arctic). The new species is the shallowest of the exclusively deep-sea torquaratorids found to date, possibly an example of high-latitude emergence. On the basis of ribosomal DNA sequences and morphology, the worm is described here as the holotype of *Coleodesmium karaensis* n. gen., n. sp. It is most similar in overall body shape to the previously described enteropneust genus *Allapasus*, but is uniquely characterized by a tubular component of the proboscis skeleton ensheathing the collar nerve cord. Additionally, within the proboscis, the sparseness of the musculature of *C. karaensis* clearly distinguishes it from the much more muscular members of *Allapasus*. The holotype is a female bearing about a dozen embryos on the surface of her pharyngeal region, each recessed within a shallow depression in the dorsal epidermis. The embryos, ranging from late gastrula to an early stage of coelom formation, are a little more than 1 mm in diameter and surrounded by a thin membrane. Each embryo comprises an external ectoderm of monociliated cells (not arranged in obvious ciliated bands) and an internal endo-mesoderm; the blastopore is closed. In the most advanced embryos, the anterior coelom is starting to constrict off from the archenteron. *Coleodesmium karaensis* is the first enteropneust (and indeed the first hemichordate) found brooding embryos on the surface of the mother's body.

Received 20 April 2013; accepted 2 October 2013.

* To whom correspondence should be addressed. E-mail: osbornk@si.edu

Introduction

The phylum Hemichordata is divided into two classes: Pterobranchia and Enteropneusta. Pterobranchs, represented by about 30 described species, are found from littoral to continental slope depths, whereas enteropneusts, with about 100 described species, live predominantly in the littoral zone (Hyman, 1959) but have occasionally been found in the deep sea. By the end of the twentieth century, the following three deep-living enteropneusts had been described, one in each of the established families of the class: *Glandiceps abyssicola* Spengel, 1893 (family Spengelidae, 4570 m), *Glossobalanus tuscarorae* Belichov, 1971 (family Ptychoderidae, 8100 m), and *Saxipendium coronatum* Woodwick and Sensenbaugh, 1985 (family Harrimaniidae, 2478 m).

The number of deep-living enteropneusts recently increased markedly with the description of an additional harrimaniid, *Saxipendium implicatum* Holland *et al.*, 2012a (3034 m) and six new species in the newly recognized family Torquaratoridae. The latter are *Torquarator bullocki* Holland *et al.* 2005 (1901 m), *Tergivelum baldwinae* Holland *et al.*, 2009 (3952 m), *Allapasus aurantiacus* Holland *et al.*, 2012b (2994 m); *Tergivelum cinnabarinum* Priede *et al.*, 2012 (2493 m), *Allapasus isidis* Priede *et al.,* 2012 (2622 m), and *Yoda purpurata* Priede *et al.,* 2012 (2622 m). Smith *et al.* (2005), Holland *et al.* (2005, 2009, 2012b), Anderson *et al.* (2011), Osborn *et al.* (2012), and Priede *et al.* (2012) discussed the ecology of torquaratorid enteropneusts. All known members of the family have been found living epibenthically on the surface of the deep-sea floor,

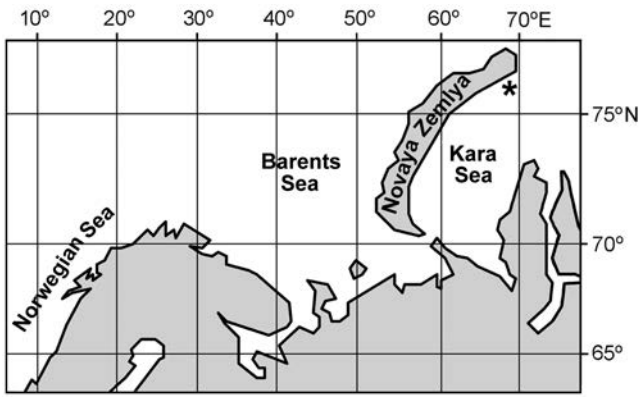

Figure 1. Map showing the collection site (at asterisk) of the holotype of *Coleodesmium karaensis* n. gen. n. sp.

although some individuals of *Allapasus aurantiacus* are known to burrow shallowly. Moreover, most, and possibly all, torquaratorids can ascend into the water above the sea floor and drift from one place to another.

Here, we use ribosomal DNA sequence and morphology to characterize an acorn worm from the Russian Kara Sea as new genus and species: *Coleodesmium karaensis* within the family Torquaratoridae. The holotype, collected from a depth of about 350 m (the shallowest for any known torquaratorid), is a female with developing embryos adhering to her epidermal surface. This is the first clear instance of external brooding ever found in the phylum Hemichordata.

Materials and Methods

In the autumn of 2011, a single acorn worm was recovered from a Sigsbee trawl during cruise 59 of the R/V *Akademik Mstislav Keldysh*. The specimen was collected at station 5051 (Fig. 1, asterisk), which sampled the floor of the Kara Sea, near the north end of the Novaya Zemlya Trough (Russian Arctic). The trawling depth ranged from 340 to 351 m. After reaching the deck, the freshly collected worm (which had lost about a third of its posterior end) was photographed under xenon strobe illumination and then divided into a minor and a major portion. The former was fixed in 95% ethanol for molecular analysis and the latter was fixed in 10% formalin in seawater for morphological study.

Genomic DNA was obtained by AutoGenprep965 proteinase K/phenol extraction (AutoGen, Inc., Holliston, MA). The amplification and sequencing of partial *16S* and complete *18S* rDNA were according to Osborn *et al.* (2012). The sequences from the Kara Sea enteropneust were approximately 500 base pairs of *16S* rDNA (GenBank KC907711) and about 1700 base pairs of *18S* rDNA (GenBank KC907710). The sequences used in our analysis are enumerated in Table 1. Sequences were aligned with MuSCLE 3.6 (Edgar, 2004) as implemented in Geneious 6.0.5 (Biomatters, Auckland, NZ). The best-fit model (GTR+G+I) was chosen using jModelTest (Posada, 2008). A 95% majority rule consensus tree for hemichordates (40 million generations) was constructed from concatenated, but unlinked nucleotide sequences (with no regions excluded) in MrBayes 3.2.1 run on the Smithsonian Institution's *Hydra* cluster in replicate. AWTY (Wilgenbusch *et al*., 2004) was used to determine if a sufficient number of generations had been completed for posterior probabilities to stabilize, as well as to determine the amount of required burn-in before inferences from the Markov Chain Monte Carlo data sets were made. The first 10K trees were removed as burn-in (20 million generations), leaving 10K trees for inference (20 million generations). Clades containing replicate individuals for a single species are labeled only a single time in the resulting tree with a triangle whose length represents the branch lengths within the clade. Maximum likelihood analyses were run using RAxML-MPI parallels version (Stamatakis, 2006) on the Smithsonian Institution's Hydra cluster. One thousand replicate best-tree searches were run and 1000 standard bootstraps. Searches were run using both the GTR+G+I and GRT+G models with no differences found between the results. Node support is expressed as posterior probability, bootstrap at respective nodes. Poorly supported nodes (<95% pp) were collapsed.

For morphological study, the formalin-fixed portion of the specimen was photographed before being embedded in Paraplast wax for histological sectioning. Serial 12-m sections were stained in 0.1% aqueous azure A (Spicer, 1963). In Paraplast-embedded tissue, larger oocytes and embryos tend to shatter during sectioning. Therefore, small samples from the pharyngeal region of the holotype were embedded in Spurr's resin, sectioned at 4 mm with a glass knife, and stained in aqueous 0.1% azure A with 0.1% sodium borate added. Serial sections of these tissue samples included two early embryos. Two additional embryos were studied by scanning electron microscopy (SEM). Each was detached from the mother's body, dehydrated in an ethanol series, critical-point dried using CO_2, mounted on stubs with double-sided tape, sputter-coated with a gold-palladium mixture, and imaged by SEM. After SEM photography, the specimens were embedded in Spurr's resin and serially sectioned.

Results

Taxonomy

Phylum Hemichordata Bateson, 1885.

Class Enteropneusta Gegenbaur, 1870.

Family Torquaratoridae Holland *et al.*, 2005 (as re-diagnosed in Osborn *et al.*, 2012).

Genus *Coleodesmium* n. gen. Type and only species: *Coleodesmium karaensis* sp. n.

Table 1

Specimen and sequence identification

	18S	*16S*	Voucher	Citation
Torquaratoridae				
Yoda purpurata (I171-36a)	JN886757	JN886740	NHMUK 2011.5	Osborn *et al.*, 2012
Yoda purpurata (I171-36b)	JN886758	JN886741	NHMUK 2011.6	Osborn *et al.*, 2012
Yoda purpurata (I174-43a)	JN886759	JN886742	NHMUK 2011.9	Osborn *et al.*, 2012
Genus B sp. 1 (T879-A8)	JN886760	EU520500	SIO-BIC H11	Osborn et al., 2012/Holland *et al.*, 2009
Genus B sp. 1 (T879-A10)	EU520513	EU520501	SIO-BIC H12	Holland *et al.*, 2009
Genus B sp. 1 (D176-A1)	JN886761	JN886744	SIO-BIC H15	Osborn *et al.*, 2012
Genus B sp. 1 (D176-A5)	JN886762	JN886745	SIO-BIC H16	Osborn *et al.*, 2012
Genus B sp. 1 (D176-A2)	JN886763	JN886746	SIO-BIC H17	Osborn *et al.*, 2012
Genus B sp. 2 (T1013-A8)	EU520514	EU520502	SIO-BIC H13	Holland *et al.*, 2009
Genus B sp. 2 (T1011)	EU520515	EU520503	SIO-BIC H14	Holland *et al.*, 2009
Genus B sp. 2 (D177-A28)	JN886764	JN886747	SIO-BIC H18	Osborn *et al.*, 2012
IFREMER Enteropneust	EU728438	EU728431	na	Cannon *et al.,* 2009
Genus C sp. 1 (T886-A4)	EU520511	EU520499	SIO-BIC H10	Holland *et al.*, 2009
Genus C sp. 1 (T1012-A8)	EU520510*	EU520498	SIO-BIC H9	Holland *et al.*, 2009
Genus C sp. 1 (D80-A2)	JN886768	JN886751	SIO-BIC H19	Osborn *et al.*, 2012
Coleodesmium karaensis n. gen. & sp.	**KC907710**	**KC907711**	**SIO-BIC H27**	**This paper**
Allapasus aurantiacus (T438)	JN886765	JN886748	SIO-BIC H20	Osborn *et al.*, 2012
Allapasus aurantiacus (D98-pc66)	JN886767	JN886750	na	Osborn *et al.*, 2012
Allapasus isidis (I174-43b)	JN886766	JN886749	NHMUK 2011.7	Osborn *et al.*, 2012
Tergivelum baldwinae (T1094)	EU520509	EU520497	SIO-BIC H8	Holland *et al.*, 2009
Tergivelum baldwinae (T10781)	JN886772	EU520495	MNHN E24	Osborn *et al.*, 2012/Holland *et al.*, 2009
Tergivelum cinnabarinum (I163-17)	JN886769	JN886752	NHMUK 2011.2	Osborn *et al.*, 2012
Tergivelum cinnabarinum (I165-24)	JN886770	JN886753	NHMUK 2011.3	Osborn *et al.*, 2012
Tergivelum cinnabarinum (I168-28)	JN886771	JN886754	NHMUK 2011.4	Osborn *et al.*, 2012
Ptychoderidae				
Balanoglossus carnosus a	D14359	na	na	Wada & Satoh, 1994
Balanoglossus carnosus b	JF900489	na	MCZ DNA103790	Worsaae *et al.*, 2012
Balanoglossus clavigerus	na	EU728425	na	Cannon *et al.,* 2009
Glossobalanus berkeleyi	EU728435	EU728426	na	Cannon *et al.,* 2009
Glossobalanus minutus	AF119089	na	MCZ DNA100058	Giribet *et al.,* 2000
Ptychodera bahamensis a	AF236802	na	na	Cameron *et al*., 2000
Ptychodera bahamensis b	JF900485	JX855285	MCZ DNA101771/4	Worsaae *et al.*, 2012
Ptychodera bahamensis c	JF900486	na	MCZ DNA103686	Worsaae *et al.*, 2012
Glossobalanus minutus	AF119089	na	MCZ DNA100058	Giribet *et al.,* 2000
Ptychodera flava a	AF278681	EU728428	na	Winchell *et al.,* 2002/Cannon *et al.,* 2009
Ptychodera flava b	EU728436	EU728429	na	Cannon *et al.,* 2009
"Ptychoderid sp. Tampa"	AF278685	EU728427	na	Winchell *et al.*, 2002/Cannon *et al.,* 2009
Unknown Family				
"Tornaria larva"	EU728438	EU728430	na	Cannon *et al.,* 2009
Spengelidae				
Glandiceps hacksi	JN886773	JN886755	HUM-HEMI-001	Osborn *et al.,* 2012
Glandiceps abyssicola	KC776731	KC776732	SIO-BIC H28	Holland *et al.,* 2013
Harrimaniidae				
Harrimania planktophilus	AF236799	EU728421	na	Cameron et al., 2000/Cannon *et al.,* 2009
Harrimania kupffferi	JF900487	JX855286	MCZ DNA103688	Worsaae *et al.*, 2012
Meioglossus psammophilus	JF900488	JX855287	ZMUC-ENP-1	Worsaae *et al.*, 2012
Protoglossus koehleri	EU728432	EU728420	na	Cannon *et al.,* 2009
Saccoglossus bromophenolosus	AF236801	na	na	Cameron *et al*., 2000
Saccoglossus kowalevskii	L28054	na	na	Turbeville *et al*., 1994
Saccoglossus pusillus	AF236800	EU728422	na	Cameron *et al*., 2000/Cannon *et al*., 2009
Saxipendium coronatum	EU728433	EU728423	na	Cannon *et al.,* 2009
Saxipendium coronatum	EU520505*	EU520493	SIO-BIC H4	Holland *et al.*, 2009
Saxipendium implicatum (D176-A11)	JN886774	JN886756	SIO-BIC H21	Osborn *et al.*, 2012

Continued

Table 1 *(Continued)*

	18S	*16S*	Voucher	Citation
Pterobranchia				
Cephalodiscus densus	EU728439	na	na	Cannon *et al.,* 2009
Cephalodiscus gracilis	AF236798	na	na	Cameron *et al*., 2000
Cephalodiscus hodgsoni	EU728441	na	na	Cannon *et al.,* 2009
Cephalodiscus nigrescens	EU728440	na	na	EU728440
Rhabdopleura normani	U15664 *	na	na	Halanych, 1995
Echinodermata				
Asteriodea, *Asterias forbesii*	DQ060776	DQ297073	AMCC 113321	Janies, 2005 unpublished
Crinoidea, *Bathycrinus* sp.	AY275891	na	D1425	Cohen *et al.*, 2004
Crinoidea, *Neogymnocrinus richeri*	AY275895	na	D1363	Cohen *et al.,* 2004
Echinoidea, *Aspidodiadema jacobi*	DQ073780	DQ073734	na	Smith *et al*., 2006
Holothuroidea, *Parastichopus californicus*	DQ777084	DQ777096	AMCC 113282	Janies, 2005 unpublished
Ophiuroidea, *Ophioderma brevispinum*	DQ060803	DQ297103	na	Janies, 2005 unpublished

* Partial sequence.

Etymology: The generic name derives from Greek *koleos*, "sheath," combined with *desmos*, "cord," in recognition of the diagnostic anatomical feature described in the next section.

Generic diagnosis: Part of the proboscis skeleton is a tubular sheath immediately surrounding the collar nerve cord for most of its length; the sheath is four to five times thicker than the extracellular basal lamina described around the collar cords of other enteropneusts.

Coleodesmium karaensis n. sp. (Figs. 3–5). Holotype (female) collected by the benthos team of the P. P. Shirshov Institute of Oceanology on 1 October 2011 during cruise 59 of the R/V *Akademik Mstislav Keldysh* at station 5051 (latitude 75.81°N–75.83°N, longitude 68.99°E–69.01°E) in the Novaya Zemlya Trench, Kara Sea, Russian Arctic. The collection was by Sigsbee trawl, at a depth between 340 and 351 m. Histological sections are conserved in the Scripps Institution of Oceanography Benthic Invertebrate Collection as SIO-BIC-H27. There are no paratypes.

Specific diagnosis: The same as for the genus.

Etymology: the species name, *karaensis*, is a latinized adjective referring to the Kara Sea, where the holotype was collected.

Phylogenetic analysis

Coleodesmium karaensis n. gen n. sp. is clearly a member of the deep-sea family Torquaratoridae (Fig. 2). *Coleodesmium karaensis* n. gen. n. sp. is genetically most closely related to another new species that was originally designated "genus C" by Osborn *et al.* (2012). Gross morphology, as seen on remotely operated vehicle video (Osborn *et al.,* 2012, fig. 1J) supports the idea of these being closely allied species, but the nature of the relationship cannot be determined without careful morphological examination of a specimen of genus C sp. 1. Genus C sp. 1 was collected off Oregon on three separate occasions (Osborn *et al*., 2012), but none of those specimens were properly photo-documented or fixed to allow morphological description. There is moderate support for a close relationship between *Tergivelum, Allapasus,* genus C, and *Coleodesmium* (Fig. 2). The genetics and anatomical features of the Kara Sea enteropneust (described below) were sufficiently different from other known torquaratorids to justify naming it *Coleodesmium karaensis* n. gen. n. sp.

External anatomy of holotype

Figure 3A shows a dorsal view of the portion of the freshly collected holotype recovered in the trawl. The recovered part of the body before fixation was 6.3 cm long and comprised a proboscis (Pr), collar (Co), and about two-thirds of the trunk (Tr); the posterior part of the hepatic intestinal region and the entire post-hepatic intestinal region were missing. All body regions of the fresh specimen were translucent and almost colorless (at most, lightly tinged with a lavender color).

Before fixation, the proboscis was dome-shaped (0.9 cm long by a maximum width of 1.2 cm) with longitudinal grooves mid-dorsally and mid-ventrally. The collar (0.5 cm long by 1.4 cm wide) was characterized by a transverse opaque stripe (Fig. 3A, white arrowhead) and had a longitudinal groove mid-dorsally that deepens and widens posteriorly. The recovered portion of the trunk was 4.8 cm long by a maximum width of 1.3 cm. All along either side of the trunk, lateral wings arose and curled dorsally, such that their edges were apposed at a mid-dorsal seam (Fig. 3A, black arrowhead). In the pharyngeal region of the trunk, cream-colored oocytes and embryos were clearly visible through the translucent body wall (some examples are indicated by arrows in Fig. 3A). The appearance of the holotype after formalin fixation is shown in Figures 3B–D. The boxes in Figure 3B indicate which regions were prepared histologically. Figure 3C shows the gill pores running on either side

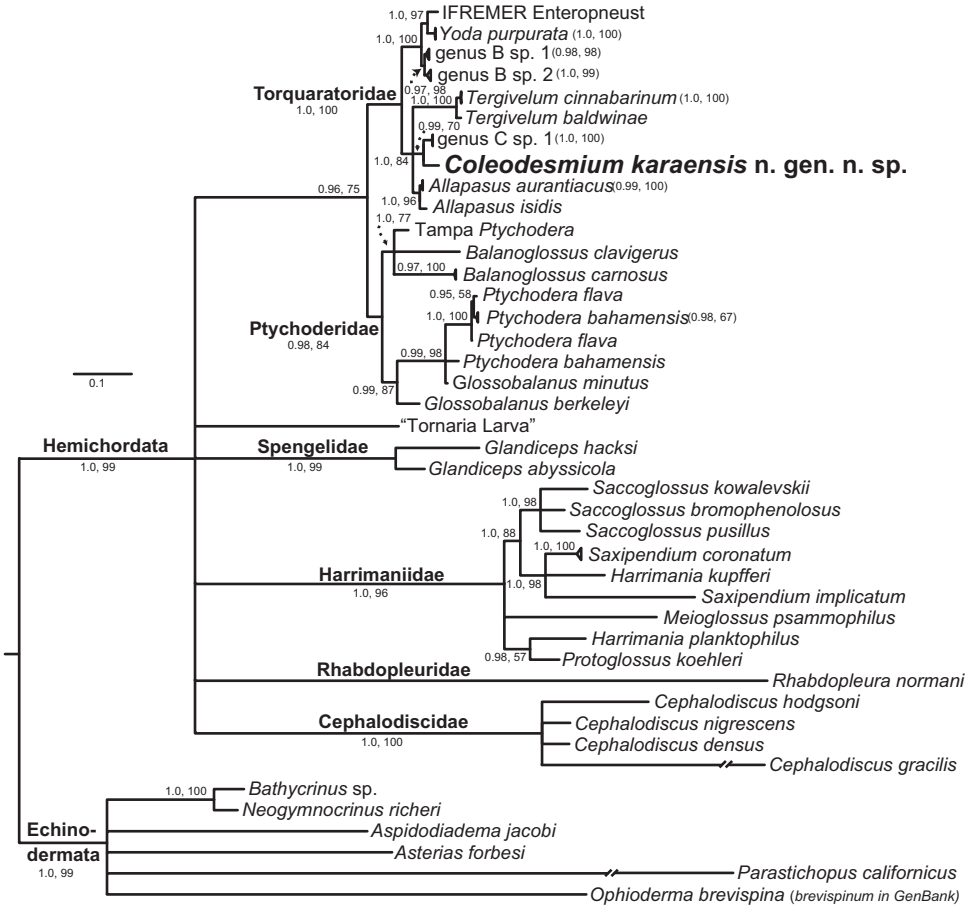

Figure 2. Phylogenetic analysis of phylum Hemichordata based on concatenated, unlinked *16S* and *18S* rDNA sequences. This is a 95% majority rule consensus tree from the final 40-million-generation Bayesian analysis. At the top left, the scale bar indicates the number of substitutions per nucleotide site. Branches with less than 0.95 posterior probability were collapsed, and species with more than one exemplar sequence are shown as cartooned clades (triangles whose width indicates genetic distance within the clade; see Table 1 for number of individuals included in each). Node support is shown as posterior probability, ML bootstrap (from the final RAxML analysis using the GTR+G model with 1000 best tree searches and 1000 bootstrap replicates).

of the dorsal nerve cord in the pharyngeal region of the trunk after the removal of the lateral wings, and the arrowhead in Figure 3D shows the prominent mid-ventral groove that runs along the ventral side of the trunk.

Internal anatomy of holotype

Some of the tissues of the holotype were damaged during capture and fixation. In addition, the abundant mucus in the epidermal cells swelled during histological processing, and large amounts ruptured outward onto the microscope slide or inward into the subepidermal tissue, especially in the proboscis. A cross section through the proboscis (Fig. 4A) shows the dorsal and ventral grooves. Internally, the proboscis is filled with a loose mesh of smooth muscles and connective tissue fibers. Part of the mesh is relatively condensed and organized into a thin, horizontally oriented sheet (Fig. 4A, arrowhead) running along most of the length of the proboscis. The proboscis musculature in *C. karaensis* is strikingly less developed than in the genus *Allapasus* and thus is a useful criterion for distinguishing between the similarly shaped worms in these two genera. No spacious protocoel, pericardial cavity, or coelomopores were detected. In the proboscis, the basal concentration of neurites of the intraepidermal nervous system comprise a neuropil that is inconspicuous except posteriorly, where it thickens on either side of the midline of the proboscis stalk (Fig. 4B, arrows; 4C, asterisk). Posteriorly, these thickened regions of neuropil merge before connecting with the dorsal collar cord.

The collar region epidermis is especially rich in mucous cells and is underlain by a sparse network of smooth muscle cells and connective tissue fibers; no coelomopores were detected. The gut in this body region is the buccal cavity (Fig. 4D, asterisk). At the anterior end of the collar, the

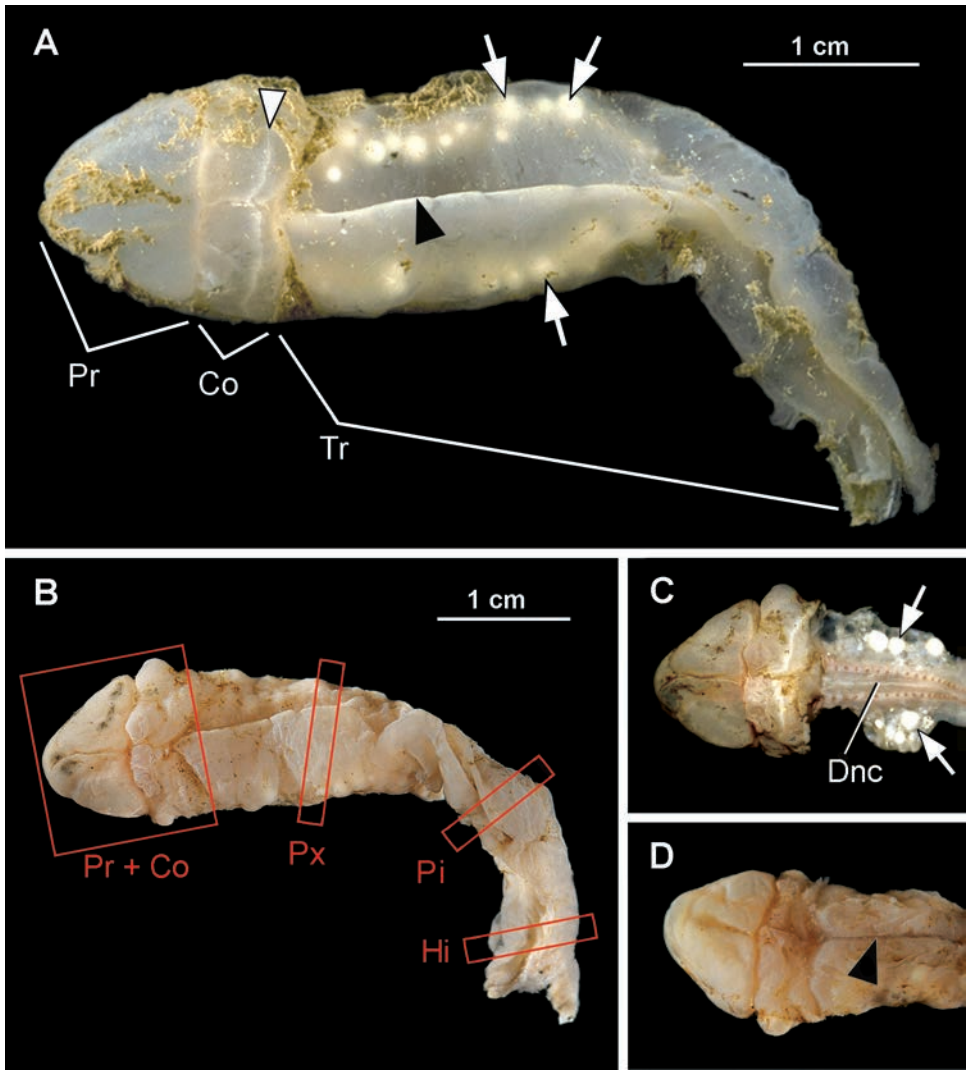

Figure 3. *Coleodesmium karaensis* n. gen. n. sp. (A) Dorsal view of the living holotype, showing proboscis (Pr), collar (Co), and trunk (Tr; posterior part missing); the white arrowhead indicates the transverse stripe on the collar; the black arrowhead indicates the mid-dorsal apposition of the left and right lateral wings accompanying the trunk; and the white arrows indicate large oocytes or embryos visible through the translucent body wall. Photo by Tina Molodtsova, P.P. Shirshov Institute of Oceanology RAS, used with permission. (B) Dorsal view after fixation indicating regions prepared as serial histological sections: proboscis + collar (Pr + Co); pharynx (Px), prehepatic intestine (Pi), and hepatic intestine (Hi). (C) Anterior part of B after removal of most of the lateral wings to expose the dorsal nerve cord of the trunk (Dnc) accompanied on either side by a row of gill pores; the arrows indicate large oocytes or embryos, respectively on or within the remnants of the lateral wings. (D) Ventral view of anterior body after fixation; along the trunk, a midventral groove (arrowhead) is conspicuous. The scale line in B is also applicable to C and D.

collar cord (Fig. 4D, arrowhead) opens to the exterior *via* a broad anterior neuropore. At this level, there is also a stomochord packed with vacuolated cells (Fig. 4D, arrow). The ventral side of the stomochord is associated with small glomeruli (Fig. 4E, arrowheads). In the mid-collar, the collar cord (Fig. 4F, arrowhead) has an inconspicuous lumen and lacks dorsal roots. Strikingly, the cord runs within a conspicuous sheath of extracellular material (especially dorsally and laterally) that can be considered an extension of the proboscis skeleton. This feature sets *C. karaensis* apart from other enteropneusts described to date. Just ventral to the stomochord are the perihaemal coeloms (Fig. 4F, asterisks) largely occupied by longitudinal muscle fibers. The stomochord (Fig. 4F, arrow) is still present ventral to the perihaemal coeloms.

Near the posterior end of the collar are plate-like elements of the proboscis skeleton (Fig. 4G, arrowheads). Unfortunately, the holotype's tissues, including the proboscis

skeleton, are damaged at this level. This means the relationships between the plate-like elements and the skeletal sheath surrounding the collar cord cannot be determined for the holotype (although it is certain that no posterior horns are present). A short distance posterior to the cross-sectional level in Figure 4G, the stomochord and perihaemal coeloms disappear, and the collar cord emerges at the posterior neuropore to continue as the dorsal nerve cord of the trunk.

In the trunk, the epidermis includes abundant mucous cells, and the mesoderm comprises a sparse network of smooth muscles and connective tissue fibers, as in the more anterior body regions. Lateral wings arise along each side of the trunk (mostly removed in Fig. 4H; damaged in Fig. 4I, but complete in Fig. 4J). The wing on either side curls dorsally and closely apposes itself to its counterpart at a mid-dorsal seam. In the pharyngeal region of the trunk, removal of the lateral wings exposes about two dozen gill pores running on either side of the dorsal nerve cord (Fig. 3C). The dorsal nerve cord is underlain by the dorsal blood vessel (Fig. 4H, arrow). Internally, the gill slits facing the pharyngeal lumen are supported by alternating primary and secondary gill bars (Fig. 4H, twin arrows) not connected by synapticles. The pharyngeal lumen is not separated into a dorsal respiratory and a ventral digestive region. The pharyngeal region of the trunk is deeply indented by a ventral groove, along which runs the ventral nerve cord underlain by the ventral blood vessel (Fig. 4H, arrowhead).

The holotype is a female (presumably *C. karaensis* has separate sexes, although no male has yet been found). The ovaries (Fig. 4H, tandem arrows) lie just beneath the epidermis covering the dorsal side of the pharyngeal region of the trunk and the concave sides of the lateral wings in the same body region. Each ovary contains a single primary oocyte that can range in diameter from a few micrometers up to about a millimeter (Fig. 5A). Each primary oocyte is characterized by a large vesicular nucleus containing a single prominent nucleolus. The largest oocytes cause an outward bulge of the epidermis but are not externalized in epidermal pouches as they are in acorn worms of the genus *Allapasus* (the latter were described by Holland *et al.*, 2012b).

In the intestinal regions of the trunk, there is still a ventral groove, but it is much shallower than that of the pharyngeal region. The lining epithelium of the prehepatic gut is corrugated into plicae (Fig. 4I). By contrast, the succeeding hepatic intestine (Fig. 4J) is characterized dorsally by larger-scale outpocketings (hepatic sacculations) oriented perpendicular to the long axis of the body (Fig. 4K). In the holotype, the only gut region containing luminal contents was the hepatic intestine. The ingested material was brownish and consisted largely of unidentifiable fibrogranular material very sparsely mixed with skeletal fragments from sponges, echinoderms, foraminifera, and diatoms. In many places, the gut contents were organized into compact spheres (Fig. 4K, arrowhead) that may possibly have been ingested fecal pellets of other organisms. As already mentioned, the trunk regions housing the posterior part of the hepatic intestine and the entire posthepatic intestine were broken off and lost during collection.

Externally brooded embryos

The female holotype of *C. karaensis* bears about a dozen embryos on the pharyngeal region of her trunk. Each is recessed in an epidermal depression (Fig. 5B) on the dorsal side of the body or on the concave (medial) side of the lateral wings. The ovoid embryos have an average diameter of about 1.2 mm (Fig. 5C). Each of the four embryos studied by embedding in Spurr's resin, by SEM, or both, comprised an ectoderm and endoderm and had a closed blastopore. Each of the thousands of ectodermal cells bore a single cilium on its outer surface (Fig. 5C–E), but no obvious ciliated bands were visible. Three of the sampled embryos were late gastrulae, with an archenteron filled with granular material, but not forming coeloms (data not shown). In the fourth embryo, an anterior coelomic space (Fig. 5F, single asterisk) was beginning to form by constriction from the archenteron (Fig. 5F, twin asterisks). A thin, single-layered membrane encloses each embryo (visible in part in Fig. 5B and intact in Fig. 5F, arrow). Whether the membrane represents a fertilization envelope or is derived from the maternal tissues is not known.

Discussion

Morphology

The proboscis skeleton of a hemichordate is a localized, conspicuous thickening of the extracellular matrix (= basal lamina) that delimits epithelia throughout the body. This material is tough but pliable after fixation. Admittedly, it is subjective just where to draw the line between skeleton and basal lamina. In *Coleodesmium karaensis*, the extracellular matrix surrounding the collar nerve is 30 μm thick (except where it thins on the ventral side); this contrasts with the thinness of the extracellular matrices associated with the collar cord of other enteropneusts, which was 4 to 7 μm, where the published pictures are large enough and clear enough to permit a good measurement. The collar does not extend beyond the cord in either direction.

Ecology

The Kara Sea (Fig. 1) experiences 24-h polar days in summer and 24-h polar nights in winter. In most years, the ice cover persists for about 9 months (October through June). Much of the Kara Sea is shallower than 50 m, and its southern region is complexly influenced by seasonal input of river water from the Russian mainland (*e.g.,* Vetrov and Romankevich, 2011; Kozlovskiy *et al.,* 2011), which

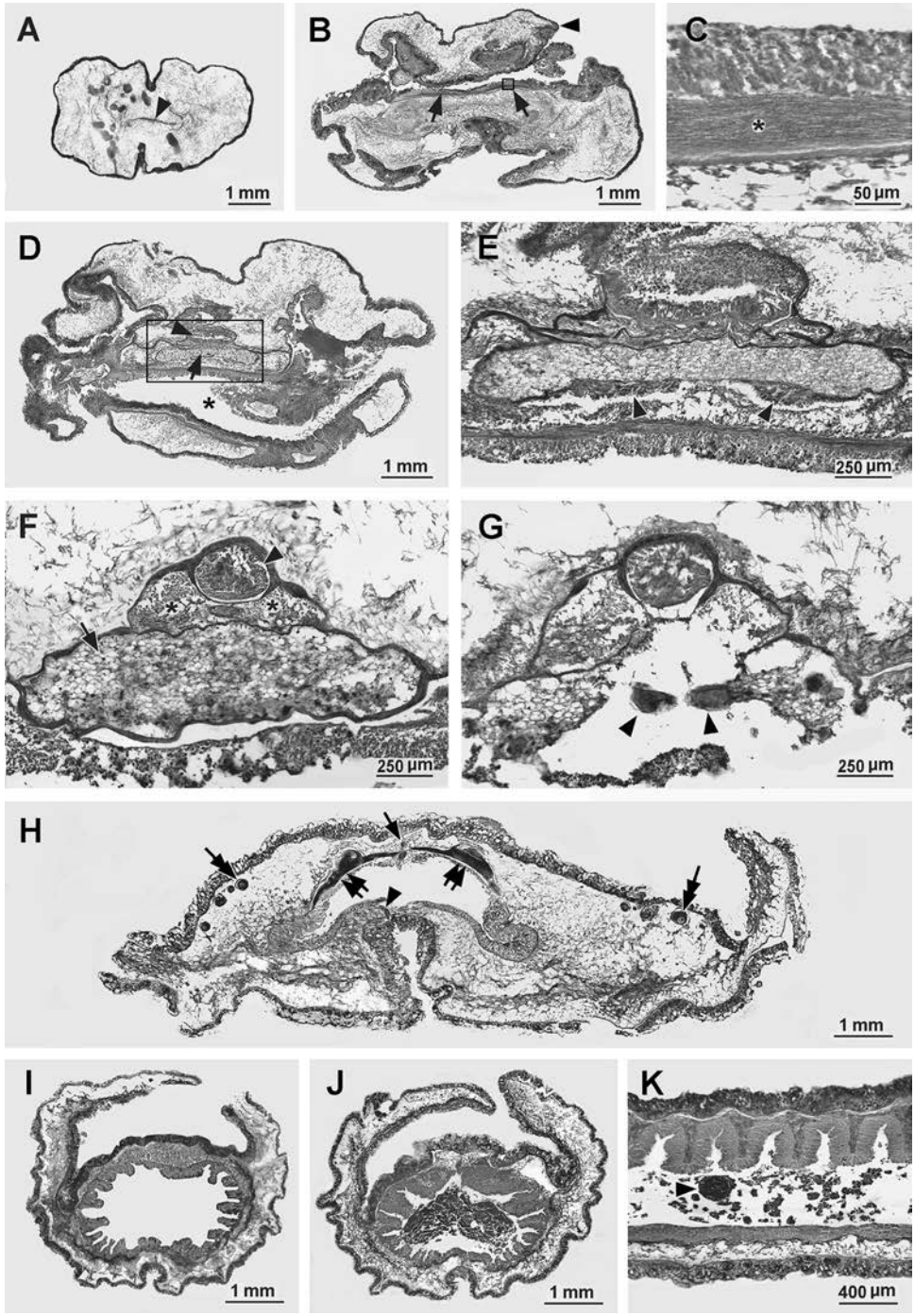

Figure 4. *Coleodesmium karaensis* n. gen. n. sp. Histological cross (A–J) or sagittal (K) sections. (A) Proboscis; arrowhead indicates relatively condensed mesh of smooth muscles and connective tissue fibers organized into a horizontally oriented sheet. (B) Anterior extremity of collar (arrowhead) overhanging the base of the proboscis stalk; arrows indicate the thickened neuropil dorsolaterally. (C) Enlargement of boxed region in B, showing detail of epidermis including basal thickening of the neuropil of the intraepidermal nervous system (asterisk). (D) Section through the buccal cavity (asterisk), collar cord (arrowhead), and stomochord (arrow) near the level of the anterior neuropore. (E) Enlargement of box in D showing inconspicuous glomeruli (arrowheads) associated with the ventral side of the stomochord. (F) Collar nerve cord (arrowhead) surrounded by an extension of the proboscis skeleton; asterisks indicate perihaemal coeloms, and arrow indicates stomochord. (G) Damaged section near posterior extremity of collar; likely plate-like portion of proboscis skeleton indicated by arrowheads. (H) Pharyngeal region of trunk showing dorsal haemal vessel (arrow), ventral haemal vessel (arrowhead), gill

strongly impacts the survivorship and other aspects of the ecology of the benthic invertebrates there (Fetzer and Arntz, 2008). By contrast, oceanographic conditions in the northwestern part of the Kara Sea fluctuate less markedly. The Novaya Zemlya Trough, which has maximum depths around 400 m, is a conspicuous feature in the northwest, running parallel to the eastern shore of Novaya Zemlya Island. The oceanographic conditions in the trough are influenced by influx of Atlantic water traversing the Barents Sea and then rounding the northern tip of Novaya Zemlya. Although there are dynamic seasonal changes in mixing of water masses in the Novaya Zemlya Trough (Loeng *et al*., 1997), the bottom water there is characterized by high salinities and low temperatures (about 0 ± 1.5 °C) all year long. At the collection site for *C. karaensis* (station 5051 during cruise 59 of the R/V *Akademik Mstislav Keldysh*), the salinity was 34.6 parts per thousand, and the water temperature was −1.4 °C at a depth of about 350 m on 1 October 2011.

The sediment recovered in the trawl with the holotype of *C. karaensis* was brown ooze and clay, which is typical of the floor of the Novaya Zemlya Trough (Galkin *et al*., 2010), and included many specimens of an epibenthic foraminifera (*Saccorhyza ramosa*). Although the collection depth of 340–351 m was considerably less than abyssal, the low temperature and perpetual darkness there are comparable to those conditions in the deep-sea generally. *Coleodesmium karaensis* is the shallowest-living torquaratorid discovered so far and is possibly an example of the high-latitude emergence that was previously noted for some other benthic animals of the Novaya Zemlya Trough by Filatova and Zenkevich (1957)—for example, the holothurian *Elpidia glacialis* Théel, 1876.

Because the holotype of *C. karaensis* was collected in a trawl, it is not known whether the worm was captured while inhabiting a burrow (like some specimens of *Allapasus aurantiacus*) or while exposed on the sediment surface like most torquaratorids described to date. The relatively poorly developed body musculature of *C. karaensis*, as compared to *A. aurantiacus*, indicates that the former might well live epibenthically and never burrow. The gut contents of *C. karaensis* were almost free of mineral grains, indicating that the worm feeds selectively, although nothing is known about the biomechanics of the deposit feeding or the identity of the foods providing major energy sources to the worm.

Reproductive biology

Coleodesmium karaensis is the first enteropneust species (and indeed the first hemichordate) ever found to brood embryos externally on the maternal surface. There is, however, an earlier report of *internal* brooding in an enteropneust by Gilchrist (1925), who published a drawing of a single advanced larva within the trunk coelom of an adult female of *Xenopleura vivipara* (family Harrimaniidae). Some enteropneust species, like *Saccoglossus pusillus* (Davis, 1908) as well as pterobranch hemichordates in the genera *Cephalodiscus* (Sciaparelli *et al.,* 2004) and *Rhabdopleura* (Lester, 1988; Sato *et al.,* 2008), retain early developmental stages in the maternal burrow or tube.

External brooding in *C. karaensis* raises a number of questions. First, do the females need to associate closely with conspecific males (presumed to exist) to effect fertilization? Second, where are the large female gametes located when they are fertilized—subepidermally or perhaps in externalized bag-like protrusions like those described for *Allapasus aurantiacus* by Holland *et al.* (2012b)? Third, one could ask whether any nutrients are transferred from the mother to the brooded developmental stages (the voluminous yolk store in the full-grown oocytes would make this seem unlikely). Fourth, how advanced is the developmental stage that hatches from the enclosing membrane and leaves the mother worm? Fifth, do the hatchlings swim in the plankton and perhaps feed there (and, if so, do they resemble large tornaria larvae) or are they lecithotrophic direct developers that do not feed? Answers to these questions would require observations on additional specimens of *C. karaensis* from one of the world's least accessible habitats.

Acknowledgments

We are indebted to the crew of the R/V *Akademik Mstislav Keldysh* and to Sergey Galkin, Andrey Vedenin, Kirill Minin, and Tina Molodtsova for help with the dredging, sorting, and photography of the freshly collected worm. Greg Rouse kindly photographed the formalin-fixed specimen, and Linda Holland constructively criticized our manuscript. Matt Kweskin kindly facilitated use of the Smithsonian's Hydra cluster. This research was supported in part by the Russian foundation of Basic Research (grant number 12-05-33049).

Figure 4. (*Continued*) bars (twin arrows), and ovaries (tandem arrows); the lateral wings that would normally arch over the pharyngeal region are largely missing. (I) Prehepatic intestine with no gut contents; lateral wings are damaged. (J) Hepatic intestine with gut contents; lateral wings are intact. (K) Parasagittal view of hepatic intestine showing hepatic sacculations dorsally; the arrowhead indicates a possible ingested fecal pellet in the gut lumen.

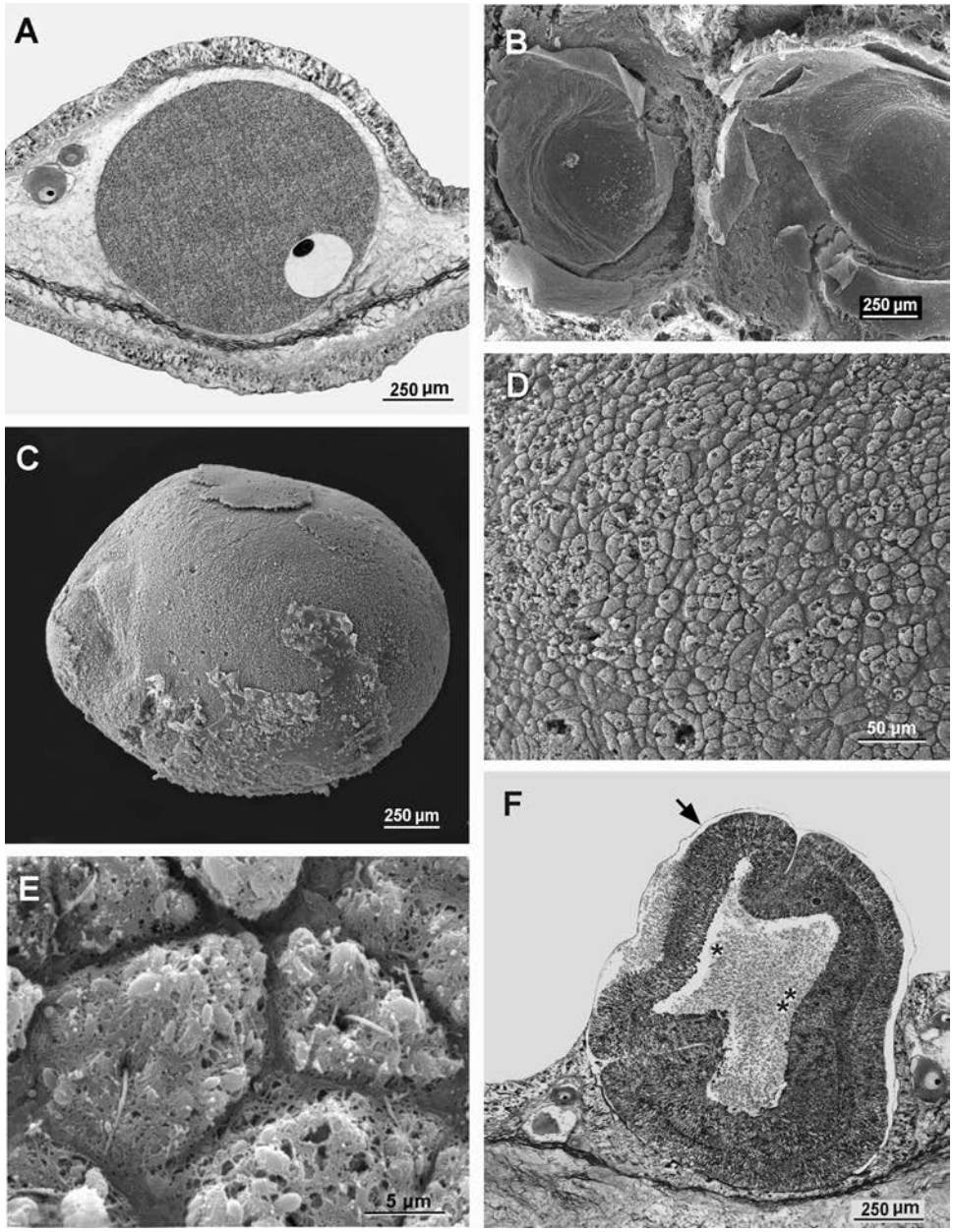

Figure 5. *Coleodesmium karaensis* n. gen. n. sp. (A) Section through part of a lateral wing (concave medial surface at top) in the pharyngeal region of the trunk, showing oocytes, one nearly maximum size. (B) Surface view of two concavities in the maternal epidermis from which brooded embryos have been removed. (C) Surface view of a gastrula removed from the maternal surface. (D) Enlarged surface view of C showing outer surface of ectoderm. (E) Enlargement of D showing outer surfaces of several cells each bearing a single cilium. (F) Section through a brooded embryo surrounded by a thin membrane (arrow) and attached to the maternal epidermis (at bottom); the embryo's archenteron (twin asterisks) is constricting off the anterior coelomic cavity (single asterisk).

Literature Cited

Anderson, T. J., R. Przeslawski, and M. Tran. 2011. Distribution, abundance and trail characteristics of acorn worms at Australian continental margins. *Deep-Sea Res. II* **58:** 970–978.

Bateson, W. 1885. Note on the later stages in the development of *Balanoglossus kowalevskii* [sic] (Agassiz), and on the affinities of the Enteropneusta. *Proc. R. Soc.* **38:** 23–30.

Belichov, D. V. 1971. Kishechnodyshashie (Enteropneusta) Kurilo-Kamchatskoj Vpadiny (Tuskarory), *Glossobalanus tuscarorae* n. sp. *Vop. Zool., Ser. 2, Kazan Pedagogical Univ.* **61:** 3–38.

Cameron, C. B., J. R. Garey, and B. J. Swalla. 2000. Evolution of the

chordate body plan: new insights from phylogenetic analyses of deuterostome phyla. *Proc. Natl. Acad. Sci. USA* **97:** 4469–4474.

Cannon, J. T., A. L. Rychel, H. Eccleston, K. M. Halanych, and B. J. Swalla. 2009. Molecular phylogeny of Hemichordata, with updated status of deep-sea enteropneusts. *Mol. Phylogenet. Evol.* **52:** 17–24.

Cohen, B. L., N. Ameziane, M. Eleaune, and B. Richer de Forges. 2004. Crinoid phylogeny: a preliminary analysis. *Mar. Biol.* **144:** 605–617.

Davis, B. M. 1908. The early life-history of *Dolichoglossus pusillus* Ritter. *Univ. Calif. Publ. Zool.* **4:** 187–226 + pl. IV-VIII.

Edgar, R. C. 2004. MUSCLE: multiple sequence alignment with high accuracy and high throughput. *Nucleic Acids Res.* **32:** 1792–1797.

Fetzer, I., and W. E. Arntz. 2008. Reproductive strategies of benthic invertebrates in the Kara Sea (Russian Arctic): adaptation of reproduction modes to cold water. *Mar. Ecol. Prog. Ser.* **356:** 189–202.

Filatova, Z. A., and L. A. Zenkevich. 1957. Kolichestvennoe raspredelenie donnoi fauny Karskogo Morya. *Tr. Vses. Gidrobiol. O-va.* **8:** 3–62.

Galkin, S. V., T. A. Savilova, L. I. Moskalev, and N. V. Kucheruk. 2010. Macrobenthos of the Novaya Zemlya Trough. *Oceanology* **50:** 982–993.

Gegenbaur, C. 1870. *Grundzüge der vergleichenden Anatomie. Zweite, umgearbeitete Auflage.* Wilhelm Engelmann, Leipzig, 892 pp.

Gilchrist, J. D. F. 1925. *Xenopleura vivipara* g. et sp. n. (Enteropneusta). *Q. J. Microsc. Sci.* **69:** 555–570.

Giribet, G., D. L. Distel, M. Polz, W. Sterrer, and W. C. Wheeler. 2000. Triploblastic relationships with emphasis on the acoelomates and the position of Gnathostomulida, Cycliophora, Platyhelminthes, and Chaetognatha: a combined approach of 18S rDNA sequences and morphology. *Syst. Biol.* **49:** 539–562.

Halanych, K. M. 1995. The phylogenetic position of the pterobranch hemichordates based on 18S rDNA sequence data. *Mol. Phylogenet. Evol*. **4:** 72–76.

Holland, N. D., D. A. Clague, D. P. Gordon, A. Gebruk, D. L. Pawson, and M. Vecchione. 2005. "Lophenteropneust" hypothesis refuted by collection and photos of new deep-sea hemichordates. *Nature* **434:** 374–376.

Holland, N. D., W. J. Jones, J. Ellena, H. A. Ruhl, and K. L. Smith. 2009. A new deep-sea species of epibenthic acorn worm (Hemichordata, Enteropneusta). *Zoosystema* **31:** 333–346.

Holland, N. D., K. J. Osborn, and L. A. Kuhnz. 2012a. A new deep-sea species of harrimaniid enteropneust (Hemichordata). *Proc. Biol. Soc. Wash.* **125:** 228–240.

Holland, N. D., L. A. Khunz, and K. J. Osborn. 2012b. Morphology of a new deep-sea acorn worm (Class Enteropneusta, Phylum Hemichordata): a part-time demersal drifter with externalized ovaries. *J. Morphol.* **273:** 661–671.

Holland, N. D., K. J. Osborn, A. V. Gebruk, and A. Rogacheva. 2013. Rediscovery and augmented description of the *H.M.S. Challenger* acorn worm (Hemichordata, Enteropneusta), *Glandiceps abyssicola*, in the equatorial Atlantic abyss. *J. Mar. Biol. Assoc. UK* **93(8):** doi: 10.1017/S0025315413000684.

Hyman, L. H. 1959. *The Invertebrates: Smaller Coelomate Groups,* Vol. 5. McGraw-Hill, New York.

Kozlovskiy, V. V., M. V. Chikina, N. V. Kucheruk, and A. B. Basin. 2011. Structure of the macrozoobenthic communities in the southwestern Kara Sea. *Oceanology* **51:** 1012–1020.

Lester, S. M. 1988. Ultrastructure of adult gonads and development and structure of the larva of *Rhabdopleura normani* (Hemichordata: Pterobranchia). *Acta Zool.* **69:** 95–109.

Loeng, H., V. Ozhigin, and B. Ardlandsvik. 1997. Water fluxes through the Barents Sea. *ICES J. Mar. Sci.* **54:** 310–317.

Osborn, K. J., L. A. Kuhnz, I. G. Priede, M. Urata, A. V. Gebruk, and N. D. Holland. 2012. Diversification of acorn worms (Hemichordata, Enteropneusta) revealed in the deep sea. *Proc. R. Soc. B* **279:** 1646–1654.

Posada, D. 2008. jModelTest: phylogenetic model averaging. *Mol. Biol. Evol.* **25:** 1253–1256.

Priede, I. G., K. J. Osborn, A. V. Gebruk, D. Jones, D. Shale, A. Rogacheva, and N. D. Holland. 2012. Observations on torquaratorid acorn worms (Hemichordata, Enteropneusta) from the North Atlantic with descriptions of a new genus and three new species. *Invertebr. Biol.* **131:** 244–257.

Sato, A., J. D. D. Bishop, and P. W. H. Holland. 2008. Developmental biology of pterobranch hemichordates: history and perspectives. *Genesis* **46:** 587–591.

Sciaparelli, S., R. Cattaneo-Vietti, and P. Mierzejewski. 2004. A "protective shell" around the larval cocoon of *Cephalodiscus densus* Anderson, 1907 (Graptolithoidea, Hemichordata). *Polar Biol.* **27:** 813–817.

Smith, A. B., D. Pisani, J. A. Mackenzie-Dodds, B. Stockley, B. L. Webster, and D. T. Littlewood. 2006. Testing the molecular clock: molecular and paleontological estimates of divergence times in the Echinoidea (Echinodermata). *Mol. Biol. Evol.* **23:** 1832–1851.

Smith, K. L., N. D. Holland, and H. A. Ruhl. 2005. Enteropneust production of spiral fecal trails on the deep-sea floor observed with time-lapse photography. *Deep-Sea Res. I* **52:** 1228–1240.

Spengel, J. W. 1893. *Fauna und Flora des Golfes von Neapel und der angrenzenden Meeres-Abschnitte. Herausgegeben von der zoologischen Station zu Neapel. 18, Monographie: Enteropneusten.* Friedländer, Berlin. 756 pp + 37 pl.

Spicer, S. S. 1963. Histochemical differentiation of mammalian mucopolysaccharides. *Ann. NY Acad. Sci.* **106:** 379–388.

Stamatakis, A. 2006. RAxML-VI-HPC: Maximum Likelihood-based Phylogenetic Analyses with thousands of taxa and mixed models. *Bioinformatics* **22:** 2688–2690.

Théel, H. 1876. Note sur l'*Elpidia*, genre nouveau du groupe des holothuries. *Bih. K. Svensk. Vet. Akad. Handl.* **4 (4):** 1–7.

Turbeville, J. M., J. R. Schulz, and R. A. Raff. 1994. Deuterostome phylogeny and the sister group of the chordates: evidence from molecules and morphology. *Mol. Biol. Evol.* **11:** 648–655.

Vetrov, A. A., and E. A. Romankevich. 2011. Genesis of organic matter in the Kara Sea bottom sediments. *Oceanology* **31:** 608–615.

Wada, H., and N. Satoh. 1994. Phylogenetic relationships among extant classes of echinoderms, as inferred from sequences of 18S rDNA, coincide with relationships deduced from the fossil record. *J. Mol. Evol.* **38:** 41–49.

Wilgenbush, J. C., D. L. Warren, and D. L. Swofford. 2004. AWTY: A system for graphical exploration of MCMC convergence in Bayesian phylogenetic inference. [Online]. Available: http://ceb.csit.fsu.edu/awty [2013, October 8].

Winchell, D. J., J. Sullivan, C. B. Cameron, B. J. Swalla, and J. Mallatt. 2002. Evaluating hypotheses of deuterostome phylogeny and chordate evolution with new LSU and SSU ribosomal DNA data. *Mol. Biol. Evol.* **19:** 762–776.

Woodwick, K. H., and T. Sensenbaugh. 1985. *Saxipendium coronatum*, new genus, new species (Hemichordata: Enteropneusta): the unusual spaghetti worms of the Galápagos hydrothermal vents. *Proc. Biol. Soc. Wash.* **98:** 351–365.

Worsaae, K., W. Sterrer, S. Kaul-Strehlow, A. Hay-Schmidt, and G. Giribet. 2012. An anatomical description of a miniaturized acorn worm (Hemichordata, Enteropneusta) with asexual reproduction by paratomy. *PLoS ONE* **7(11):** e48529.